Applied Radiation and Isotopes 127 (2017) 103–108

Contents lists available at ScienceDirect

Applied Radiation and Isotopes

journal homepage: www.elsevier.com/locate/apradiso

Synthesis and stimulated luminescence property of $Zn(BO_2)_2$:Tb^{3+}

G. Cedillo Del Rosario[a,b], E. Cruz-Zaragoza[a,*], M. García Hipólito[b], J. Marcazzó[c], J.M. Hernández A.[d], H. Murrieta S[d]

[a] Instituto de Ciencias Nucleares, Universidad Nacional Autónoma de México, A. P. 70-543, 04510 México D.F., México
[b] Posgrado en Ciencia e Ingeniería de Materiales, Instituto de Investigaciones en Materiales-UNAM, A. P. 70-360, 04510 México D.F., México
[c] Instituto de Física Arroyo Seco-CIFICEN, CONICET-UNCPBA, Pinto 399, 7000 Tandil, Argentina
[d] Instituto de Física, Universidad Nacional Autónoma de México, A. P. 20-364, 01000 México D.F., México

ARTICLE INFO

Keywords:
Metaborate
Thermoluminescence
Radioluminescence
Terbium
Dosimetry

ABSTRACT

Zinc borate, $Zn(BO_2)_2$, doped with different concentrations of terbium (0.5–8 mol%) was synthesized and polycrystalline samples were characterized by Scanning Electron Microscopy and X-Ray Diffraction. The $Zn(BO_2)_2$ was formed in the pure samples sintered at 750 and 800 °C which has the body centered cubic structure, and a ZnB_4O_7 primitive orthorhombic phase was present. The thermoluminescent intensity was dependents on the thermal treatment (250–500 °C) and also on the impurity concentration. The linear dose-response was obtained between 0.022–27.7 Gy and 0.5–50 Gy when the samples were exposed to beta and gamma radiation, respectively. The complex structure of the glow curves was analyzed by the Computerized Glow Curve Deconvolution method. The kinetics parameters were calculated assuming the general order kinetics model describing accurately the TL process. The glow curves of Tb^{3+}-doped zinc borate phosphor were well deconvolved by six glow peaks. Zinc borate with 8 mol% of impurity concentration exhibited an intense radioluminescent emission. The radioluminescent spectra show their maximum bands at 370, 490, 545 and 700 nm related to the terbium ion in the zinc borate. These obtained results suggest that the terbium doped zinc borate is a promising phosphor for use in radiation dosimetry because of its high TL sensitivity to the ionizing radiation.

1. Introduction

Since the initial proposal by Schulman et al. (1967), the lithium metaborate ($Li_2B_4O_7$:Mn) was accepted as a material dosimeter for ionizing radiation by using their thermoluminescent property. Also various alkaline earth (Li, Mg, Ca, Sr, Ba) based on tetraborate doped with different ions have been synthesized to use in radiation dosimetry. (Schulman et al., 1967; Paun et al., 1977; Takenaga et al., 1980; Sabharwal and Sangeeta, 1998; Soramasu and Yasuno, 1996; Furetta et al., 2000; Santiago et al., 2001; Guarneros-Aguilar et al., 2013).

Because of their atomic number is very close to that of soft tissue equivalent (Z_{eff}=7.4) material, large linearity of dose-response, and good thermoluminescent (TL) sensitivity to gamma, beta and neutron radiation makes tetraborates an interesting phosphor to develop and to investigate on its TL and optically stimulated luminescent (OSL) properties for radiation dosimetry in general. However, the linearity of the dose-response, its TL sensitivity, and variability of the TL features within a batch as well as among different batches has been observed (Driscoll et al., 1981, 1986). Following, some efforts were made in increase the TL sensitivity of the tetraborates by using different dopant and co-dopants as efficient luminescent centers (Takenaga et al., 1980; Lorrain et al., 1986; Prokić, 2000). Copper ion, instead of manganesium, was used with successful to increase the TL intensity due to its emission spectrum at about 360 nm in the lithium borate (Prokić, 2001). Furthermore, the Li ion as co-dopant enhanced the TL sensitivity in the tetraborates phosphors doped with Mn, Dy, or Tm ions. Recently some authors have been reported a new zinc tetraborate compound prepared by different methods (Li et al., 2007, 2008; Annalakshmi et al., 2011, 2014; Kucuk et al., 2013, 2015, 2016) and subject to different annealing procedures. It is important to mention that the annealing is a process of a heating material to a given temperature and then cooling. The TL intensity of the dosimetric peak (~300 °C) in thulium (Tm) doped zinc tetraborate (Annalakshmi et al., 2014) was about twenty times higher than that of commercial LiF:Mg,Ti (TLD-100) dosimeter. When the $Zn(BO_2)_2$ borate was doped with Ce^{3+} ions and exposed to beta radiation the main glow peak was at about 230 °C and increases with increasing doses (Kucuk et al., 2016). In the case of terbium (Tb) doped zinc borate the TL and photoluminescence emission

* Corresponding author.
E-mail address: ecruz@nucleares.unam.mx (E. Cruz-Zaragoza).

http://dx.doi.org/10.1016/j.apradiso.2017.05.018
Received 16 May 2017; Accepted 22 May 2017
Available online 24 May 2017

bands were at about 490, 543, 584 and 620 nm, and they were associated to Tb^{3+} ions when the samples were excited with wavelength 261 nm (Li et al., 2007). In addition, the borate phosphor has an important advantages over the lithium fluoride (LiF:Mg,Ti) that has a complex glow curve structure and it requires complicated thermal treatment for re-use. However, a disadvantage of the zinc borates is their high effective atomic number ($Z_{eff} \approx 22.4$). In the case of the phosphors with high Z_{eff}, such as $CaSO_4$ ($Z_{eff} = 15.3$) and CaF_2 ($Z_{eff} = 16.3$), have a dependence of the photon energies, i.e., at photon energy below about 100 keV the TL response becomes significantly greater than that at higher energies. In the case of environment or medical applications, the possible dependence on the photon energy may be improved by using adequate filters (Pradhan et al., 1992; Lakshmanan et al., 1986).

Other important property of some phosphors and natural material for dating is the radioluminescence (RL) (Santiago et al., 1998; Krbetschek and Trautmann, 2000; Santiago et al., 2001) and this property also is present in our Tb^{3+} doped zinc borate. The luminescence stimulated response and emission in real-time from the natural and synthetic samples during irradiation. It has been recently investigated mainly for dating purposes (Trautmann et al., 1999; Krbetschek and Trautmann, 2000), also the RL has been proposed to be uses for radiation protection and dosimetry using some phosphor materials (Petö and Kelemen, 1996; Aznar, 2005). In this phenomenon, the real-time measurement is possible to carry out, it is the main advantage on the TL method.

This work has motivation in the potentialities of the borate for the application in radiation dosimetry at low doses and searching their TL and RL characteristics. Also the zinc borate is in the framework of the develop phosphor material to radiation detector in our laboratory. The purpose of this work was to synthesize the pure and terbium doped zinc borate by the solvent evaporation method obtaining a higher TL sensitivity, and to analyze its TL properties under gamma and beta radiation, and the RL property under beta radiation too. The influence of sintering temperature on the zinc borate compound is also reported.

2. Materials and methods

2.1. Synthesis of zinc borate

The zinc borate doped and undoped have been synthesized by the solvent evaporation method. The reagents zinc acetate $(CH_3CO_2)_2Zn{\cdot}2H_2O$ purity 98.9% and boric acid (H_3BO_3) purity 99.999% were mixed in the stoichiometric ratio (1:2). The terbium chloride ($TbCl_3{\cdot}6H_20$) of 99.9% purity as aqueous solution, in the required concentration was added to obtain an impurity content ranging from 0.5 to 8 mol%. The reagents thoroughly stirred in a flask on a hot plate at 250 °C for 15 min and then raised to 400 °C during 16 min. After stirring and desiccation the mixture material was sintered in air at 750, 800, 900 and 950 °C temperatures for different periods of time (15–18 h) and the porous molten mass was obtained. An alumina crucible in a Barnstead/Thermolyne furnace type 1500 Thermo Scientific were used. The molten mass was then cooled to room temperature, crushed, and sieved to obtain powder less than 74 μm and 74–420 μm particle sizes. These particles sizes were selected in order to obtain the best TL intensity and well defined peaks along of the glow curves.

2.2. Sample analyses

The characterization of the zinc borate powder samples was carried out by using X-ray diffraction (XRD) to analyze the effect of doping on the structure of the undoped sample and identifying the phases in the samples. The X- ray analysis was made using a Bruker AXS D8-Advance diffractometer with Cu-Kα (30 kV, 0.5° min^{-1}, $10° < 2\theta < 80°$) radiation of wavelength 0.15418 nm. The morphological structure, detailed mapping and chemical composition of the borate samples were analyzed using Scanning Electron Microscopy (SEM) (JEOL JSM-7600F, model Stereoscan 440) coupled to an Energy Dispersive Spectroscopy (EDS) detector model Pentafet ISIS link.

2.3. Thermoluminescent measurements

All thermoluminescent (TL) measurements were carried out on double aliquots of 6.00 ± 0.01 mg powder samples using a Harshaw model 3500 TLD reader. The glow curves were obtained by a constant heating rate of 2 °C/s, from room temperature up to 450 °C and under nitrogen atmosphere in order to avoid the spurious TL signals. Samples were exposed to gamma photon and beta radiation, using a ^{60}Co Gammacell-200 AECL-Nordion with 0.1689 Gy/min and with a 3.7×10^8 Bq ophthalmic $^{90}Sr/^{90}Y$ beta-source with 0.022 Gy/min dose rate, respectively. The irradiations were made at room temperature. The zinc borate samples were placed in acrylic plates with 3 mm thickness to have the electronic equilibrium condition during irradiation.

3. Results and discussion

3.1. Effect of sintering temperature and X-ray diffraction patterns

The zinc borate (ZnB_2O_4) was doped with terbium ion at different concentration (0.5, 1, 2, 4, 8 mol%) and this powder material was sintered at 600, 750, 800, 900 and 950 °C during different period of time (15–18 h) in order to obtain the best crystallization of the samples, and different phases formed at these temperatures were observed. Sintering at 600 °C for 16 h, the undoped zinc borate was an amorphous phase. Then the polycrystalline powder samples of undoped and terbium-doped zinc borate were sintered at higher temperatures.

At 750 °C temperature, the formation of $Zn(BO_2)_2$ cubic phase combined with ZnB_4O_7 orthorhombic was obtained. The best preparation of undoped zinc borate was obtained at 800 °C for 18 h and at 900 °C during 16 h, because the single $Zn(BO_2)_2$ phase was obtained. At these sintered temperatures prevail the zinc borate phase with 100% crystallinity. The XRD patterns for crystal structure and phase identification of the $Zn(BO_2)_2$ were obtained.

The X-ray difractrograms of the undoped samples, sintered at 750 and 800 °C, shown the evidence of the $Zn(BO_2)_2$ has the body centered cubic (bcc) structure and ZnB_4O_7 primitive orthorhombic phase of the crystal system. Finally, at 950 °C sintered temperature, the XRD identified a single phase material when a porcelain crucible was used, but not so in the case of alumina crucible. In this last case, three phases were identified: 46.78% of $Zn(BO_2)_2$, 8.34% of hexaboron oxide (B_6O) was formed and 8.34% of corundum (Al_2O_3) phase. This last phase is due to that material could not be separated cleanly from the base of the alumina crucible. Figs. 1 and 2, shown the XRD patterns from the terbium doped zinc borate and from the standard JCPDC card number 039–1126 (Figs. 1a and 2a). Zinc borate was crystallized into a bcc structure with lattice parameter of a = 7.473 Å and space group *Im3m*. Figs. 1b and 2b, shown the X-ray diffraction patterns of $Zn(BO_2)_2$ pure and terbium doped [4 mol%] samples, respectively. It was choose the sample $Zn(BO_2)_2{:}Tb^{3+}$ [4 mol%] because their better TL response. Besides, zinc borate doped with terbium [4 mol%] and sintered at 800 °C for 16 h, has a defined structural morphology as discussed by SEM-EDS analysis. In this preparation samples, the main phase was Zn $(BO_2)_2$ which contributes about 80% of the intensity in the X-ray pattern, also the zinc-borate-ZnB_4O_7, zinc borate-alpha-$Zn_5B_4O_{11}$/$5ZnO{\cdot}2B_2O_3$, and zinc hydroxide-epsilon-$Zn(OH)_2$ phases were found. It was observed that the XRD patterns showed a decrease in the crystallinity of $Zn(BO_2)_2{:}Tb^{3+}$ with increasing the dopant concentration (0.5–8 mol%). This behavior was related to the defect formation that comes from to the charges of $TbCl_3{\cdot}6H_2O$ dopant as well as impurity phases present in the final product of zinc borate material.

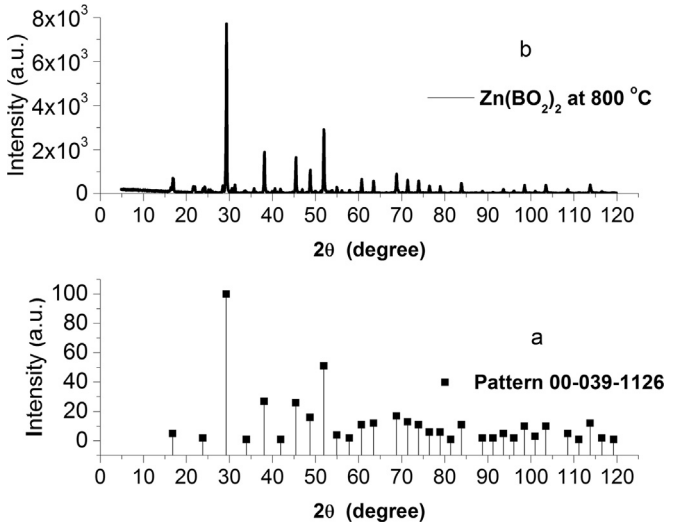

Fig. 1. XRD pattern of the $Zn(BO_2)_2$, (a) corresponding to JCPDC data file 039-1126, and (b) pure $Zn(BO_2)_2$ with 800 °C sintering temperature during 18 h.

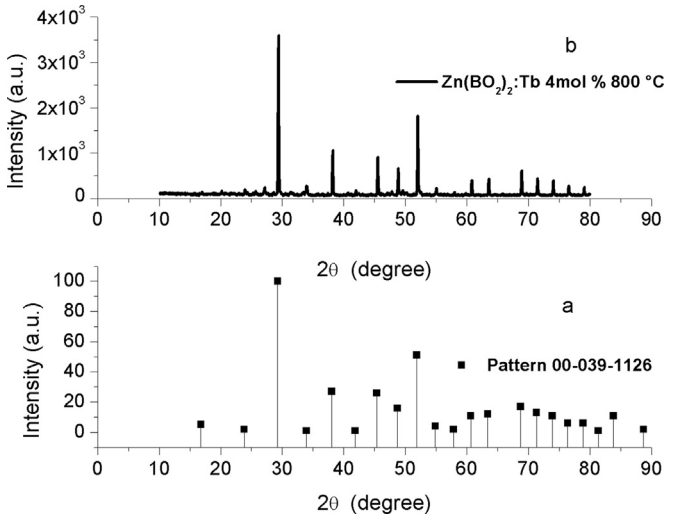

Fig. 2. XRD pattern of the $Zn(BO_2)_2$, (a) from JCPDC data file number 039-1126, and (b) $Zn(BO_2)_2$ doped with $TbCl_3{\cdot}6H_2O$ [4 mol%] and sintered at 800 °C during 16 h.

3.2. SEM micrographs and EDS spectrum analyses

The surface of the $Zn(BO_2)_2$:Tb^{3+} [4 mol%] samples was analyzed by SEM-EDS. The images have been obtained with magnifications of 500 to 50,000 with lower secondary electron and the low-angle backscattered electron (LABE) detector coupled to the SEM equipment. SEM image showed grains with cubic and orthorhombic structures (Fig. 3a), which were well defined at a magnification of X500. These grains with size of microns there are clumps of zinc, boron, terbium and oxygen elements that are present in the samples. The chemical composition of the $Zn(BO_2)_2$:Tb^{3+} [4 mol%] was determined using the EDS detector. The main elements were oxygen (49.8 at%), boron (34.6 at%) and zinc (12.73 at%), also terbium impurity was determined in the samples at about 2.87 at%. It is important to mention, various scanning by EDS on the surface of the block structure (Fig. 3b) reveal the zinc borate atomic composition was formed with terbium at 1.08 at %, and the oxygen, boron, and zinc, at 52.80, 31.46, 14.67 at%, respectively. The significant atomic percent (1.08–2.87) of terbium present in the zinc borate may be ascribed to the aggregation of the impurity in the material and might depends on the impurity concentration used. It was observed, when the zinc borate was doped with terbium at the lower concentration (0.5 mol%), the impurity was not detected by EDS, however the TL signal was sensible to this last terbium concentration in the phosphor. Also the sintering temperature is an important factor to growth the grains and to provide a crystalline material and by the subsequent annealing treatment help to the impurity diffusion in the lattice phosphor to obtain the same initial condition to the TL experiments. Finally, particles with higher contrast were observed in the SEM image (Fig. 3a and b), they have the same chemical composition to the block structure but different atomic percent of the composition; oxygen was present at 56.98 at%, boron and zinc at 23.63 and 17.8 at%, respectively, and Tb^{3+} impurity at 1.6 at% were detected.

3.3. Thermoluminescence response of $Zn(BO_2)_2$ exposed to gamma and beta radiation

Thermoluminescence glow curves of the borates samples were analyzed at different annealing temperature (250–500 °C) because the TL intensity depends on the thermal treatment and on the impurity concentration too. As can be seen from Fig. 4, the highest TL intensity was obtained at 400 °C annealing temperature. This temperature (400 °C) was used subsequently in the pre-irradiation annealing and readout cycle of the TL measurements of the samples. The structure or shape of the glow curves by different annealing of $Zn(BO_2)_2$:Tb^{3+} was similar for both gamma and beta irradiation (Fig. 5). The thermoluminescent (TL) intensity was dependent on the thermal treatment of the samples and also on their impurity concentration. The grain size influenced the TL intensity of the terbium doped zinc borate samples. The TL intensity of the second peak height (152 °C) of the large particles selected for the samples (74–420 μm) was approximately 2.9 times more intense than that of the glow curve belonging to 74 μm particles samples. Similar behavior to the dose-response was observed, i.e. the total area under the glow curves increased with the grain size particles increases of the samples. The glow curves of zinc borate doped with terbium showed a TL glow peak at about 91 °C which disappeared after 2 h of storage in darkness and at room temperature or under a thermal bleaching at 120 °C due to thermal detrapping. Then it was necessary to perform a post-irradiation annealing procedure at 120 °C during 5 min in order to eliminate this low temperature peak. It is important to mentioning that this annealing does not affect the main TL glow peak at 152 °C. Taken this into account, the fading was carried out over a period of 30 days using a post-irradiation annealing with 120 °C to eliminate the glow peak at low temperature with fast fading. The samples were irradiated with gamma radiation at 5 Gy. At the end of 24 h no fading was observed, while at the end of 30 days the decay of the TL signal was 8.3%.

The reproducibility of the TL signals from the $Zn(BO_2)_2$:Tb^{3+} was carried out by ten times sequentially irradiating at the same dose (5 Gy) and taking readout for the samples using the same temperature (120 °C) as post-irradiation annealing temperature. In this context, the standard deviation of 4.3% was obtained. Furthermore, the lower detection limit (D_{LDL}) defined as three times the standard deviation of the zero-dose reading was calculated. The average and standard deviation of ten readout with zero-dose were carried out and a $D_{LDL} = 0.01$ Gy was found.

The dose-response was linear between 0.5 and 50 Gy when the samples were irradiated with ^{60}Co in Gammacell-200 irradiator. At less doses, the TL dose-response was obtained between 0.02 and 27 Gy from $Zn(BO_2)_2$:Tb^{3+} samples under beta radiation of $^{90}Sr/^{90}Y$ source. Fig. 6 shows the integrated TL response as a function of the beta and gamma doses in the investigated dose range of the zinc borate samples. As can be seen, a good linearity is observed within the whole dose-response measured. In the inset of the figure, the glow curves dependence of sample $Zn(BO_2)_2$:Tb^{3+} irradiated with beta radiation from 0.02 up to 27 Gy is shown.

The peaks in the glow curves at different beta doses were similarly to those in the TL curves of the zinc borates samples irradiate with

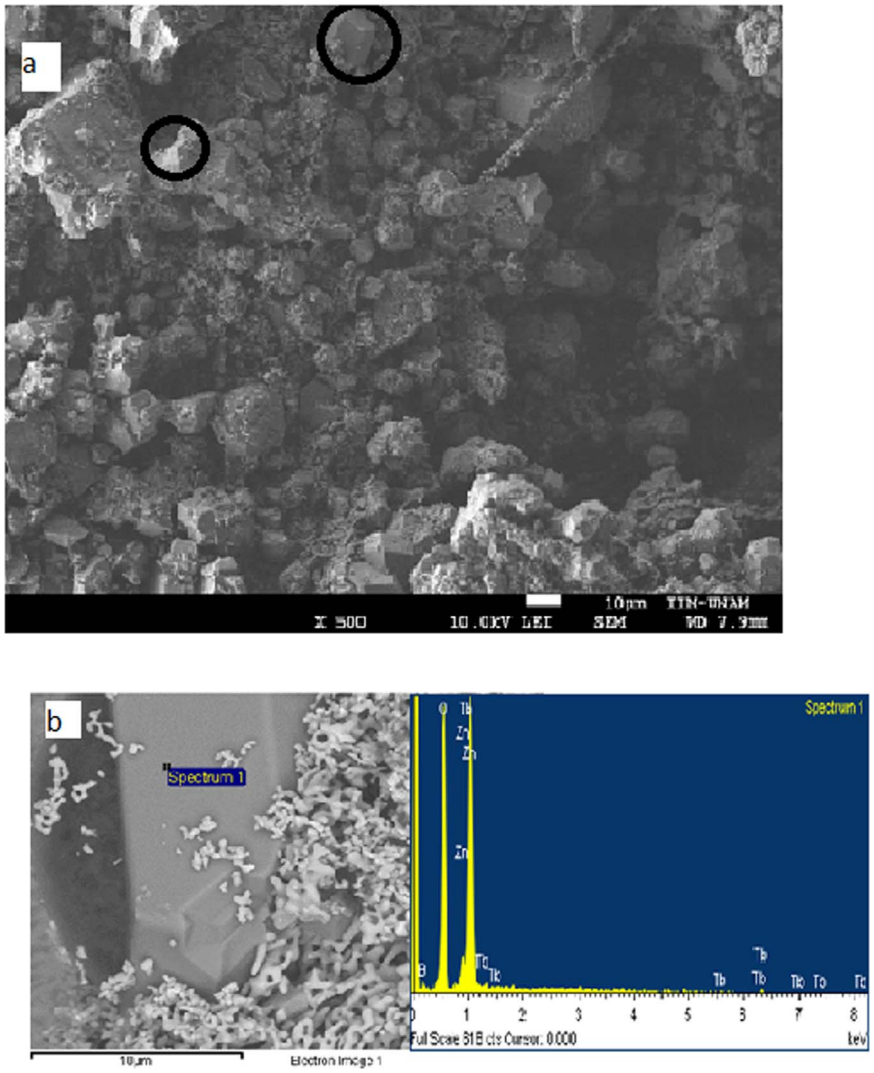

Fig. 3. (a) Scanning electron micrograph of $Zn(BO_2)_2$:Tb^{3+} [4 mol%], magnification of X500. (b) The cubic and orthorhombic structures (in circles) were observed, EDS analysis was carried out on the surface of the block structure.

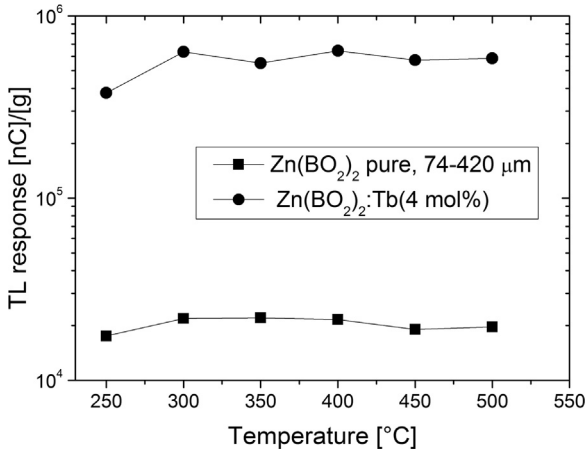

Fig. 4. TL response at different annealing temperature (250–500 °C), pure sample and Tb^{3+} [4 mol%] doped zinc borate. Both samples exposed to 5 Gy gamma dose of ^{60}Co.

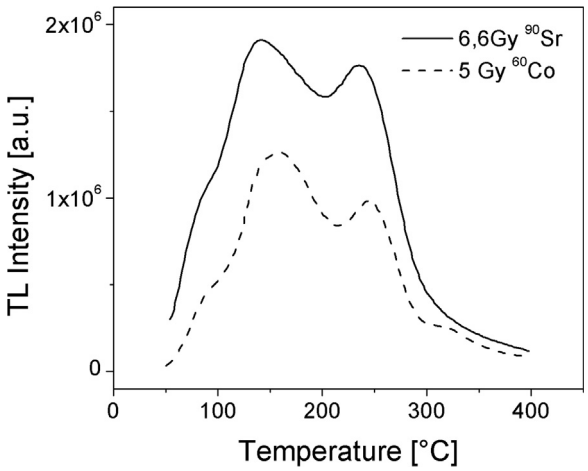

Fig. 5. Glow curves of $Zn(BO_2)_2$:Tb^{3+} [4 mol%] irradiated with a beta dose of 6.6 Gy (solid line) and with a gamma dose of 5 Gy (dash line). The samples received 400 °C annealing temperature.

gamma doses. It was related to the same kind of traps and defects are present during recombination mechanisms in the terbium doped zinc borate material. All glow curves of the zinc borate samples showed a complex structure that was solved in overlapped glow peaks. The analysis of the glow curves was carried out by a computerized glow curve deconvolution program (CGCD) assuming the general order kinetics (GOK) model (May and Partridge, 1964). TL glow curves of $Zn(BO_2)_2$:Tb^{3+} [4 mol%] irradiated with 5 Gy of gamma dose and

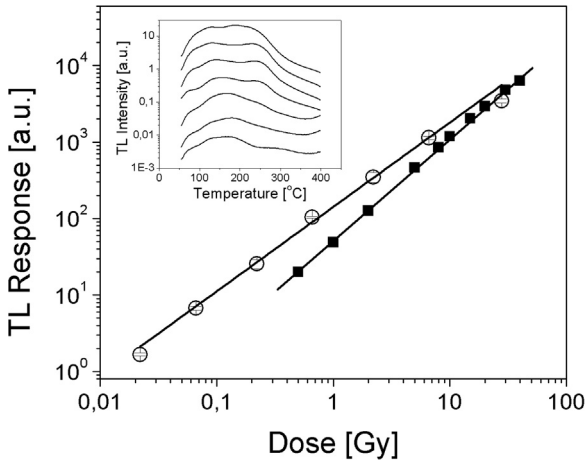

Fig. 6. Integrated TL response of $Zn(BO_2)_2$:Tb^{3+} [4 mol%] as a function of beta dose from 0.02 up to 27 Gy (open circle) and as a function of gamma dose from 0.5 up to 50 Gy (black square), respectively. Each symbol represents the average of three measurements. In the inset, glow curves of $Zn(BO_2)_2$:Tb^{3+} [4 mol%] at different beta doses.

without annealing treatment were well deconvolved by six glow peaks. Goodness of fit was evaluated by means the figure of merit (FOM) (Horowitz and Yossian, 1995) given by

$$FOM = \frac{\sum_{i=1}^{N} |I_{fit}(T) - I_{exp}(T)|}{\sum_{i=1}^{N} |I_{exp}(T)|} * 100\%$$

where $I_{exp}(T)$ and $I_{fit}(T)$ are the experimental and fitted glow curves, respectively. A set of parameters is acceptable if the FOM is less than 5%. In this work, a very acceptable FOM of 1.1% was obtained.

The main peak at 154 °C in the experimental glow curves was solved by deconvolution in two overlapped peaks (142 and 179 °C) (Table 1), and slightly increase value of the activation energy (0.95 eV) was determined for the second peak (179 °C). The activation energy (E) values increase as maximum temperature (Tm) peak was increased along of the glow curve (88–385 °C), and the kinetic order (b) was between first and second order (1.5–2.1). The frequency factor values ($s \sim 10^{10}$–10^{12} s^{-1}) were in the expected range of the solid state matter (10^5–10^{13} s^{-1}). The positions of the maximum of the overlapped peaks were in agreement with those observed in the experimental glow curves.

3.4. Radioluminescence and RL emission spectra of $Zn(BO_2)_2$:Tb^{3+}

The RL-sensitivity and spectral emission of different concentration of terbium doped $Zn(BO_2)_2$ under beta radiation are analyzed, for the first time, in order to investigate the terbium participation in the luminescence emission and to assess their possible use for in-vivo and in real time dosimetry.

Radioluminescence curves were measured as a function of time during beta irradiation. All the samples were irradiated at RT with the $^{90}Sr/^{90}Y$ beta-source and the light emitted by the samples was collected by means of a φ = 1 mm communication grade optical fiber and projected onto a Sens-Tech P25PC-02 photon counting PMT. RL spectra were recorded by means of an Acton Research SP-2155 0.150 m monochromator featuring the same Sens-Tech P25PC-02 PMT. Spectra were measured within the wavelength range of 300–700 nm and at a rate of 1 nm seg^{-1}. A resolution of approximately 5 nm was obtained.

Table 1
Kinetics parameters (FOM < 5%) of terbium-doped zinc borate phosphor, obtained by CGCD deconvolution program assuming the general order kinetics (GOK) model.

Peak	Tm [K]	E [eV]	s [s^{-1}]	b
1	361 (88 °C)	0.83	1.96×10^{12}	2.1
2	415 (142 °C)	0.91	1.33×10^{11}	2.1
3	452 (179 °C)	0.95	5.96×10^{10}	2.1
4	518 (245 °C)	1.13	7.74×10^{10}	1.5
5	588 (315 °C)	1.16	4.86×10^{9}	1.5
6	658 (385 °C)	1.20	9.04×10^{9}	1.9

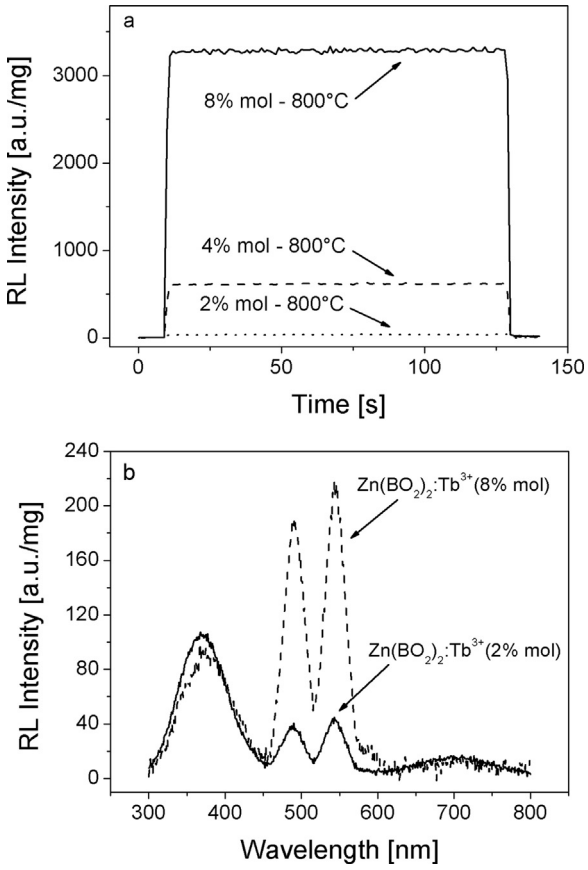

Fig. 7. (a) RL curves from $Zn(BO_2)_2$ doped with different Tb^{3+} concentrations [2,4,8 mol %] and sintered at 800 °C, (b) RL spectra of samples doped with 2 and 8 mol% of terbium impurity.

Fig. 7a shows the RL intensity as function of time and under beta irradiation of zinc borate samples doped with different concentrations of terbium [2,4,8 mol%] and sintered at 800 °C. All samples have been normalized by sample weight. Among the terbium doped samples, Zn $(BO_2)_2$:Tb^{3+} [8 mol%] shows the most intense RL emission. Besides, no change in RL sensitivity during irradiation was observed. In order to obtain information about recombination centers that are involved in the recombination process, RL spectra of two concentration of terbium [2,8 mol%] under beta irradiation are shown in Fig. 7b. It is apparent that characteristic bands of Tb^{3+} are observed for the three different concentrations. In particular, the peaks centered at 480 and 540 nm can be assigned to the $^5D_4 \rightarrow {}^7F_6$ and $^5D_4 \rightarrow {}^7F_5$ transitions of Tb^{3+}. The broad band between 300 and 450 nm can be attribute to the host because the ratio between peaks centered at 480 and 540 nm and the broad band between 300 and 450 nm increase with terbium impurity concentration.

4. Conclusions

In this work the TL properties under gamma and beta radiation, and RL properties under beta radiation, of undoped and several concentrations of Tb^{3+} doped zinc borates samples have been reported. The Zn $(BO_2)_2$ was synthesized by solvent evaporation method at different temperature and sintered during different period of time. The X-ray difractrograms of the pure and doped samples showed the cubic (bcc)

phase in this material. The chemical composition determined by SEM-EDS analysis corresponds to the terbium doped borate compound. The TL intensity was dependent on the thermal treatment and also on the impurity concentration. The higher TL intensity of the signals was presented at 400 °C annealing temperature during 0.5 h. The low peak (88–92 °C) in the glow curve was erased by using a post-irradiation annealing at 120 °C. The deconvolution method showed two peaks are involved in the main glow peak (~154 °C) of the glow curves. The maximum of the deconvolved peaks and the kinetics parameters are in agreement with those of the experimental glow peaks and according to the range values in solid state matter, respectively.

TL characterization of $Zn(BO_2)_2$:Tb^{3+} [4 mol%] under gamma and beta radiation showed a good linear response, acceptable reproducibility and no fading (at the end of 24 h) if it is performed a post-irradiation annealing procedure at 120 °C during 5 min without affecting the main glow peak centered at 152 °C. Besides, the RL response at different impurity concentration was studied and it was found that Zn $(BO_2)_2$:Tb^{3+} [8 mol%] showed the highest RL emission in the RL response during irradiation. Taking into account these TL and RL properties, $Zn(BO_2)_2$:Tb^{3+} appears to be a promising detector deserving further investigations. The broad band of the RL spectra between 300 and 450 nm can be attribute to the host and increase with terbium impurity concentration. Finally, the peaks centered at 480 and 540 nm were ascribed to the $^5D_4 \rightarrow {}^7F_6$ and $^5D_4 \rightarrow {}^7F_5$ transitions of Tb^{3+} impurity in the lattice.

Acknowledgments

We would like to acknowledge the fine work of Adriana Tejeda, Omar Novelo and Josué Romero (IIM-UNAM) by characterizing the metaborate material with XRD and SEM/EDS. Also thank Francisco García and Benjamín Leal (ICN UNAM) for carried out the irradiation of the samples. The first author (Guillermina Cedillo) acknowledges financial support from CONACYT Mexico for the doctoral fellowship (202043). This work was partially supported by PAPIIT-DGAPA UNAM under projects number IN115814 and IN112617.

References

Annalakshmi, O., Jose, M.T., Amarendra, G., 2011. Dosimetric characteristics of manganese doped lithium tetraborate - An improved TL phosphor. Radiat. Meas. 46, 669–675.

Annalakshmi, O., Jose, M.T., Madhusoodanan, U., Subramanian, J., Venkatraman, B., Amarendra, G., Mandal, A.B., 2014. Thermoluminescence dosimetric characteristics of Thulium doped ZnB_2O_4 phosphor. J. Lumin. 146, 295–301.

Aznar, M.C., 2005. Real-Time In Vivo Luminescence Dosimetry in Radiotherapy and Mammography Using Al_2O_3:C. Risø-PhD-12(EN), Denmark.

Driscoll, C.M.H., Mundy, S.J., Elliot, J.M., 1981. Sensitivity and fading characteristics of thermoluminescent magnesium borate. Radiat. Prot. Dosim. 1 (2), 135–137.

Driscoll, C.M.H., Barthe, J.R., Oberhofer, M., Busuoli, G., Hickman, C., 1986. Annealing procedures for commonly used radiothermoluminescent materials. Radiat. Prot. Dosim. 14 (1), 17–32.

Furetta, C., Prokic, M., Salamon, R., Kitis, G., 2000. Dosimetric characteristics of a new production of MgB_4O_7.Dy, Na thermoluminescence material. Appl. Radiat. Isot. 52, 243–250.

Guarneros-Aguilar, C., Cruz-Zaragoza, E., Marcazzó, J., Palomino-Merino, R., Espinosa, J.E., 2013. Synthesis and TL characterization of $Li_2B_4O_7$ doped with copper and manganese. AIP Conf. Proc. 1544, 70–77.

Horowitz, Y.S., Yossian, D., 1995. Computerised glow curve deconvolution: application to thermoluminescence dosimetry. Radiat. Prot. Dosim. 60, 1–114.

Kucuk, N., Kucuk, I., Cakir, M., Kaya Keles, S., 2013. Synthesis, thermoluminescence and dosimetric properties of La–doped zinc borates. J. Lumin. 139, 84–90.

Kucuk, N., Gozel, A.H., Yüksel, M., Dogan, T., Topaksu, M., 2015. Thermoluminescence kinetic parameters of different amount La-doped ZnB_2O_4. Appl. Radiat. Isot. 104, 186–191.

Kucuk, N., Kucuk, I., Yüksel, M., Topaksu, M., 2016. Thermoluminescence characteristics of $Zn(BO_2)_2$:Ce^{3+} under beta irradiation. Radiat. Prot. Dosim. 168 (4), 450–458.

Krbetschek, M.R., Trautmann, T., 2000. A spectral radioluminescence study for dating and dosimetry. Radiat. Meas. 32, 853–857.

Lakshmanan, A.R., Chandra, B., Pradhan, A.S., Supe, S.J., 1986. Application of thermoluminescence dosemeters for personnel monitoring in India. Radiat. Prot. Dosim. 17, 49–52.

Li, J., Zhang, C.X., Tang, Q., Zhang, Y.L., Hao, J.,Q., Su, Q., Wang, S.B., 2007. Synthesis, photoluminescence, thermoluminescence and dosimetry properties of novel phosphor $Zn(BO_2)_2$:Tb. J. Phys. Chem. Solids 68, 143–147.

Li, J., Zhang, C., Tang, Q., Hao, J., Zhang, Y., Su, Q., Wang, S., 2008. Photoluminescence and thermoluminescence properties of dysprosium doped zinc metaborate phosphors. J. Rare Earths 26, 203–206.

Lorrain, S., David, J.P., Visocekas, R., Marinello, G.A., 1986. A study of new preparations of radiothermoluminescent lithium borates with various activators. Radiat. Prot. Dosim. 17, 385–392.

May, C.F., Partridge, J.A., 1964. Thermoluminescent kinetics of alpha-irradiated alkali halides. J. Chem. Phys. 40, 1401–1409.

Paun, J., Iozsa, A., Jipa, S., 1977. Dosimetric characteristics of alkaline-earth tetraborates radiothermoluminescent detectors. Radiochem. Radioanal. Lett. 28 (5–6), 411–421.

Petö, Á., Kelemen, A., 1996. Radioluminescence properties of alpha-Al_2O_3 TL dosemeters. Radiat. Prot. Dosim. 65, 139–142.

Pradhan, A.S., Gopalakrishnan, A.K., Iyer, P.S., 1992. Dose measurement at high atomic number interfaces in megavoltage photon beams. Med. Phys. 19, 355–356.

Prokić, M., 2000. Effect of lithium co-dopant on the thermoluminescence response of some phosphors. Appl. Radiat. Isot. 52, 97–103.

Prokić, M., 2001. Lithium borate solid TL detectors. Radiat. Meas. 33, 393–396.

Sabharwal, S.C., Sangeeta, 1998. Effect of sodium doping on TL and optical properties of barium borate (BaB_2O_4) single crystals. J. Cryst. Growth 187, 253–258.

Santiago, M., Graseli, C., Caseli, E., Lester, M., Lavat, A., Spano, F., 2001. Thermoluminescence of SrB_4O_7:Dy. Phys. Status Solidi (a) 185 (2), 285–289.

Santiago, M., Lester, M., Caseli, E., Lavat, A., Ges, A., Spano, F., Kessler, C., 1998. Thermoluminescence of sodium borates compounds containing copper. J. Mater. Sci. Lett. 17, 1293–1296.

Soramasu, N., Yasuno, Y., 1996. Perfectly tissue equivalent TLD phosphor $Li_2B_4O_7$:Cu, Pb. In: Proceedings of the 9th International Congress IRPA, Vol. 4. Vienna, Austria. pp. 312–314.

Schulman, J.H., Kirk, R.D., West, E.J., 1967. Use of lithium borate for thermoluminescen ce dosimetry. In: Proc. Int. Conf. on Luminescence Dosimetry, US AEC Symposium series CONF-650637, Stanford University, USA. pp. 113–117.

Takenaga, M., Yamamoto, O., Yamashita, T., 1980. Preparation and characteristics of $Li_2B_4O_7$:Cu phosphor. Nucl. Instrum. Methods 175, 77–78.

Trautmann, T., Krbetschek, M.R., Dietrich, A., Stolz, W., 1999. Radioluminescence dating: a new tool for quaternary geology and archaeology. Naturwissenschaften 86, 441–444.